MITSUBISHI ELECTRIC RESEARCH LABORATORIES
http://www.merl.com

Tire-Stiffness Estimation by Marginalized Adaptive Particle Filter

Berntorp, K.; Di Cairano, S.

TR2016-147 December 12, 2016

Abstract

This paper considers longitudinal and lateral tirestiffness estimation for road vehicles, using wheel-speed and inertial measurements. The deviations from nominal stiffness values are treated as disturbances acting on the vehicle, and are included in a nonlinear vehicle model. We formulate a Bayesian approach based on particle filtering, where the tire stiffness as well as the associated uncertainty are jointly estimated together with the vehicle velocity vector, the yaw rate, and the bias components for the inertial sensors. For computational efficiency, we marginalize out the noise parameters, hence do not need to include them in the state vector. Experimental data for a double lane-change maneuver indicate that the stiffness can be estimated within a few percent of the true values.

IEEE Annual Conference on Decision and Control (CDC)

Tire-Stiffness Estimation by Marginalized Adaptive Particle Filter

Karl Berntorp[1] and Stefano Di Cairano[1]

***Abstract*— This paper considers longitudinal and lateral tire-stiffness estimation for road vehicles, using wheel-speed and inertial measurements. The deviations from nominal stiffness values are treated as disturbances acting on the vehicle, and are included in a nonlinear vehicle model. We formulate a Bayesian approach based on particle filtering, where the tire stiffness as well as the associated uncertainty are jointly estimated together with the vehicle velocity vector, the yaw rate, and the bias components for the inertial sensors. For computational efficiency, we marginalize out the noise parameters, hence do not need to include them in the state vector. Experimental data for a double lane-change maneuver indicate that the stiffness can be estimated within a few percent of the true values.**

I. Introduction

The tire–road interaction is the dominating factor in generating, or changing, the motion of a ground vehicle, and the knowledge of variables related to the tire–road interaction is essential for advanced driver-assistance systems [1]. A common way to model the tire–road relation is to assume a static relationship between force and slip. For small slip values, the force-slip relation is approximately linear. The slopes in the longitudinal and lateral directions of the tire are known as the longitudinal and lateral (cornering) stiffness, respectively. It is well known that there is a dependence between the tire stiffness and the peak road-friction coefficient [2], [3]. Furthermore, the linear approximation is widely employed in different applications; for example, the cornering stiffness is a key parameter when using the linear single-track vehicle model for control [4] and estimation [5].

Consequently, there is a rich literature on tire-stiffness estimation. The approaches in [2], [6] formulate the stiffness estimation as linear regressions, [3] uses the longitudinal dynamics to solve for the longitudinal stiffness in a nonlinear total least-squares problem, and [7] employs an observer-based technique. In [8], a sliding-mode observer and an extended Kalman filter estimate the cornering stiffness, whereas [9] exploits independent wheel actuation to estimate friction coefficient and cornering stiffness. Another approach for lateral stiffness estimation based on the planar lateral dynamics is found in [10].

This paper reports on a novel approach for jointly estimating stiffness parameters in both the longitudinal and lateral direction, the vehicle velocity vector, and the yaw rate. Since we treat both longitudinal and lateral dynamics, we increase the available information than if considering the longitudinal and lateral dynamics separated from each other, which is often done in literature. The vehicle state is not directly observed. We therefore pose the problem as a nonlinear, joint state and parameter estimation problem with wheel-speed, acceleration, and yaw-rate measurements; that is, using sensors often available in production cars. To handle the resulting nonlinear, non-Gaussian estimation problem, we propose a computationally efficient particle-filter based solution, where the stiffness parameters are considered as unknown Gaussian disturbances affecting the vehicle dynamics. Particle filters solve nonlinear non-Gaussian filtering problems by generating random state trajectories and assigning a weight to them according to how well they predict the observations [11].

A common approach to jointly estimate states and parameters is to augment the state vector and let the parameters be driven by artificial dynamics, as for example, in [8]. However, increasing the state dimension is particularly problematic for particle filters in automotive applications, where computational burden must be limited. Instead, we rely on marginalization [12] and propagation of the sufficient statistics of the noise parameters, conditioned on the estimated vehicle states, using the concept of conjugate priors [13]. The resulting estimation model has dependent process and measurement noise. We leverage a computationally efficient framework to account for this; see our companion paper [14] for a more detailed derivation. Our framework is related to [15], but extends to dependent noise sources and partially known measurement noise. Furthermore, we incorporate estimation of the inherent bias in the inertial sensors.

Notation: The notation $\boldsymbol{x} \sim \mathcal{N}(\boldsymbol{\mu}, \boldsymbol{\Sigma})$ for a column matrix $\boldsymbol{x}$ indicates that $\boldsymbol{x}$ is Gaussian distributed with mean $\boldsymbol{\mu}$ and covariance $\boldsymbol{\Sigma}$. With $\mathrm{St}(\boldsymbol{\mu}, \Upsilon, \nu)$, we mean the multivariate Student-t distribution with mean $\boldsymbol{\mu}$, scaling Υ, and ν degrees of freedom. Similarly, $\mathrm{NiW}(\boldsymbol{\mu}, \boldsymbol{\Lambda}, \nu)$ is the Normal-inverse-Wishart distribution with associated hyperparameters. The notation $\hat{\boldsymbol{z}}_{k|m}$ means the estimate of $\boldsymbol{z}$ at time index k given measurements up to time index m. Furthermore, $p(\boldsymbol{x}_{0:k}|\boldsymbol{y}_{0:k})$ is the posterior density of the state trajectory from time index 0 to time index k, given the measurement sequence.

II. Vehicle Model and Problem Statement

To get a tractable estimation problem using standard sensors only, we make certain assumptions. First, we consider normal driving conditions with moderate steering and acceleration. Second, we assume that the left and right wheel on each axle are similar in terms of stiffness. The presented framework conceptually can handle these cases, but it increases computation time and modeling complexity [16]. With these assumptions, the joint state and parameter estimation can be based on a single-track model. In the

[1]Karl Berntorp and Stefano Di Cairano are with Mitsubishi Electric Research Laboratories (MERL), 02139 Cambridge, MA, USA. Email:{karl.o.berntorp,dicairano}@ieee.org

following, F^x, F^y is the longitudinal and lateral tire force, respectively, α is the wheel-slip angle, ψ is the yaw, v^X, v^Y is the longitudinal and lateral vehicle velocity, respectively, and subscripts f, r stand for front and rear, respectively. The equations are

$$\begin{aligned} m(\dot{v}^X - v^Y\dot{\psi}) &= F_f^x\cos(\delta) + F_r^x - F_f^y\sin(\delta), \\ m(\dot{v}^Y + v^X\dot{\psi}) &= F_f^y\cos(\delta) + F_r^y + F_f^x\sin(\delta), \\ I\ddot{\psi} &= l_f(F_f^y\cos(\delta) + F_f^x\sin(\delta)) - l_rF_r^y. \end{aligned} \tag{1}$$

The longitudinal and lateral tire forces depend nonlinearly on the wheel slip λ and slip angle α, but since we assume normal driving equations, the tire forces can be expressed as

$$F^x \approx C^x\lambda, \quad F^y \approx C^y\alpha, \tag{2}$$

where C^x and C^y are the longitudinal and lateral stiffness, respectively. Furthermore, because we assume normal driving conditions, the approximations $\cos(\delta) \approx 1$, $\sin(\delta) \approx \delta$ hold. We adopt the definition of wheel slip from [17],

$$\lambda := \frac{v^X - R_w\omega}{\max\{v^X, R_w\omega\}}, \tag{3}$$

where ω is the wheel rotation rate and R_w is the effective wheel radius. The slip angles are approximated as

$$\alpha_f \approx \delta - \frac{v^Y + l_f\dot{\psi}}{v^X}, \quad \alpha_r \approx \frac{l_r\dot{\psi} - v^Y}{v^X}. \tag{4}$$

In (3), (4), since we assume normal driving, we use the velocity at the center of mass instead of the velocity at the center of the wheel. The vehicle model composed of (1)–(4) is nonlinear in v^X and contains bilinearities between states, and states and parameters. There is a benefit with considering both longitudinal and lateral dynamics, since coupling is introduced. However, this also increases computational complexity. The wheel rotation rates ω_f, ω_r and steer angle δ form the input vector $\boldsymbol{u}$, which is assumed known in the following. This is consistent with many navigation systems, where dead reckoning is used to decrease state dimension. Although the wheel rotation rates can be considered as measurements disturbed by noise, this would increase state dimension, which is highly unwanted in automotive applications, where computational load must be kept low. After introducing $\boldsymbol{x} = [v^X \; v^Y \; \dot{\psi}]^{\mathrm{T}}$ and discretizating with sampling time T_s, (1)–(4) can be compactly written as

$$\boldsymbol{x}_{k+1} = \bar{\boldsymbol{f}}(\boldsymbol{x}_k, \boldsymbol{u}_k). \tag{5}$$

A. Estimation Model

Eq. (5) can be rewritten by decomposing the stiffness into one known nominal part and one unknown part,

$$C^x \approx C_n^x + \Delta C^x, \quad C^y \approx C_n^y + \Delta C^y, \tag{6}$$

where C_n is the nominal value of the stiffness, for example, determined on a nominal surface, and ΔC is the time-varying, unknown part. We define

$$\boldsymbol{w}_k := \begin{bmatrix}\Delta C_f^x & \Delta C_f^y & \Delta C_r^y\end{bmatrix}^{\mathrm{T}} \in \mathbb{R}^{d_w}$$

as random process noise acting on the otherwise deterministic system. We assume that the noise term $\boldsymbol{w}_k$ is Gaussian distributed according to $\boldsymbol{w}_k \sim \mathcal{N}(\boldsymbol{\mu}_k, \boldsymbol{\Sigma}_k)$, where $\boldsymbol{\mu}_k$ and $\boldsymbol{\Sigma}_k$ are, in general, time varying, mean and covariance of the unknown tire stiffness. Inserting (6) into (5) allows us to write the dynamics as

$$\boldsymbol{x}_{k+1} = \boldsymbol{f}(\boldsymbol{x}_k, \boldsymbol{u}_k) + \boldsymbol{g}(\boldsymbol{x}_k, \boldsymbol{u}_k)\boldsymbol{w}_k. \tag{7}$$

In the following, we are interested in estimating both the state $\boldsymbol{x}_k$ and the parameters $\boldsymbol{\theta}_k := \{\boldsymbol{\mu}_k, \boldsymbol{\Sigma}_k\}$ of the process noise $\boldsymbol{w}_k$. One interpretation of the parameters is that the mean models the stiffness variations based on the surface type, such as asphalt or snow, and the variance models the uncertainty due to variations on a surface, or other unmodeled effects.

The measurements assumed available are the longitudinal and lateral accelerations a_m^X, a_m^Y, and the yaw rate $\dot{\psi}_m$, forming the measurent vector $\boldsymbol{y}_k = [a_m^X \; a_m^Y \; \dot{\psi}_m]^{\mathrm{T}}$. To relate $\boldsymbol{y}_k$ to the states, note that a^X and a^Y can be extracted from (1), and the yaw-rate measurement is directly related to the yaw rate. An inertial sensor typically has a bias b, which needs to be modeled for any realistic implementation. We model the bias as a random walk,

$$\boldsymbol{b}_{k+1} = \boldsymbol{b}_k + \boldsymbol{w}_{b,k}, \tag{8}$$

where $\boldsymbol{b}_k = [b_{x,k} \; b_{y,k} \; b_{\psi,k}]^{\mathrm{T}} \in \mathbb{R}^3$ are the bias terms for the acceleration vector and yaw rate, and $\boldsymbol{w}_{b,k}$ is assumed to be zero-mean Gaussian with covariance matrix $\boldsymbol{Q}$, $\boldsymbol{w}_{b,k} \sim \mathcal{N}(\boldsymbol{0}, \boldsymbol{Q})$. The characteristics of the noise source $\boldsymbol{w}_{b,k}$ can be determined from an Allan-variance analysis [18]. Thus, the measurement model can be written as

$$\boldsymbol{y}_k = \boldsymbol{h}(\boldsymbol{x}_k, \boldsymbol{u}_k) + \boldsymbol{b}_k + \bar{\boldsymbol{e}}_k \in \mathbb{R}_y^d, \tag{9}$$

where, $\bar{\boldsymbol{e}}_k = \boldsymbol{d}(\boldsymbol{x}_k, \boldsymbol{u}_k)\boldsymbol{w}_k + \boldsymbol{e}_k + \boldsymbol{w}_{b,k}$, $d_y = 3$,

$$\boldsymbol{d}(\boldsymbol{x}_k, \boldsymbol{u}_k) = \begin{bmatrix}T_s g_1(\boldsymbol{x}_k, \boldsymbol{u}_k) & T_s g_2(\boldsymbol{x}_k, \boldsymbol{u}_k) & 0\end{bmatrix}^{\mathrm{T}},$$

where g_j means the jth row of $\boldsymbol{g}$ in (7), and $\boldsymbol{e}_k$ is the Gaussian zero-mean noise from the inertial sensors, $\boldsymbol{e}_k \sim \mathcal{N}(\boldsymbol{0}, \boldsymbol{R})$, where $\boldsymbol{R}$ can be determined a priori.

Remark 1: It is possible to treat the measurement-noise parameters as unknown and include any bias terms in the mean of the measurement noise. The resulting measurement-noise parameters to be estimated would then include a combination of stiffness parameters, actual measurement noise, and bias terms. From a computational point of view, it is beneficial to treat the noise parameters from the inertial measurements as known, since these can be determined a priori. Furthermore, the characteristics of the bias can also be determined offline. This information can then be utilized for more reliable estimation of the noise parameters.

B. Observability

Observability can be analyzed by augmenting the dynamic model (5) with the stiffness parameters, model them as a random walk, and derive the observability Gramian by linearization. In our case, assuming nonzero steering angle and wheel slip, it can be shown that the Gramian is nonsingular, hence the system is weakly observable.

C. Problem Formulation

We want to jointly estimate the state vector $\boldsymbol{x}_k$, the parameters $\boldsymbol{\theta}_k := \{\boldsymbol{\mu}_k, \boldsymbol{\Sigma}_k\}$ of the Gaussian process noise $\boldsymbol{w}_k$, and the bias of the inertial sensors, $\boldsymbol{b}_k$, subject to the system model consisting of (7)–(9). We tackle this problem by approximating the joint posterior $p(\boldsymbol{b}_k, \boldsymbol{\theta}_k, \boldsymbol{x}_{0:k}|\boldsymbol{y}_{0:k})$. From the joint posterior, we can then extract the different quantities. Next, we describe a computationally efficient method for doing this joint estimation in a Bayesian framework. Since the unknown noise parameters enter both (7) and (9), the noise sources are dependent.

III. State and Tire-Stiffness Estimation

We formulate the joint estimation in a Bayesian framework as approximating the joint density $p(\boldsymbol{b}_k, \boldsymbol{\theta}_k, \boldsymbol{x}_{0:k}|\boldsymbol{y}_{0:k})$. We decompose

$$p(\boldsymbol{b}_k, \boldsymbol{\theta}_k, \boldsymbol{x}_{0:k}|\boldsymbol{y}_{0:k}) = p(\boldsymbol{b}_k|\boldsymbol{\theta}_k, \boldsymbol{x}_{0:k}, \boldsymbol{y}_{0:k}) p(\boldsymbol{\theta}_k|\boldsymbol{x}_{0:k}, \boldsymbol{y}_{0:k}) \cdot p(\boldsymbol{x}_{0:k}|\boldsymbol{y}_{0:k}). \quad (10)$$

The three densities at the right-hand side of (10) are estimated recursively. The key idea is that given the state trajectory, we can update the sufficient statistics of the unknown noise parameters. Similarly, given the parameters and the state trajectory, the posterior density of the bias simplifies considerably. However, the three densities are not computed independently from each other.

A. State Estimation

We approximate the posterior of the state trajectory with a particle filter [11] as

$$p(\boldsymbol{x}_{0:k}|\boldsymbol{y}_{0:k}) \approx \sum_{i=1}^{N} q_k^i \delta(\boldsymbol{x}_{0:k} - \boldsymbol{x}_{0:k}^i), \quad (11)$$

where $\delta(\cdot)$ is the Dirac delta function and q_k^i is the importance weight for the ith state trajectory $\boldsymbol{x}_{0:k}^i$. For simplicity, in this work we use a sequential importance resampling (SIR) based particle filter [11]. In general, the particles are sampled using a proposal distribution $\pi(\boldsymbol{x}_{k+1}|\boldsymbol{x}_{0:k}^i, \boldsymbol{y}_{0:k+1})$. For dependent noise, the weight update is [19]

$$q_k^i \propto q_{k-1}^i \frac{p(\boldsymbol{y}_k|\boldsymbol{x}_{0:k}^i, \boldsymbol{y}_{0:k-1}) p(\boldsymbol{x}_k^i|\boldsymbol{x}_{0:k-1}^i, \boldsymbol{y}_{0:k-1})}{\pi(\boldsymbol{x}_k^i|\boldsymbol{x}_{0:k-1}^i, \boldsymbol{y}_{0:k})} \quad (12)$$

where $p(\boldsymbol{y}_k|\boldsymbol{x}_{0:k}^i, \boldsymbol{y}_{0:k-1})$ is the likelihood. If the proposal is chosen to equal $p(\boldsymbol{x}_k^i|\boldsymbol{x}_{0:k-1}^i, \boldsymbol{y}_{0:k-1})$, (12) simplifies to

$$q_k^i \propto q_{k-1}^i p(\boldsymbol{y}_k|\boldsymbol{x}_{0:k}^i, \boldsymbol{y}_{0:k-1}). \quad (13)$$

Clearly, since the unknown process noise parameters affect both the measurement and prediction step (see (9))

$$p(\boldsymbol{y}_k|\boldsymbol{x}_{0:k}^i, \boldsymbol{y}_{0:k-1}), \quad (14a)$$
$$p(\boldsymbol{x}_{k+1}^i|\boldsymbol{x}_{0:k}^i, \boldsymbol{y}_{0:k}), \quad (14b)$$

the weight update will depend on the parameter estimates.

B. Parameter Estimation

From (14), knowing both the state and measurement trajectory gives full knowledge about $\bar{\boldsymbol{w}}_{0:k} = [\boldsymbol{w}_{0:k}\ \bar{\boldsymbol{e}}_{0:k}]^{\mathrm{T}}$. Thus, the posterior for $\boldsymbol{\theta}_k$ can be rewritten using Bayes' rule,

$$p(\boldsymbol{\theta}_k|\boldsymbol{x}_{0:k}, \boldsymbol{y}_{0:k}) \propto p(\bar{\boldsymbol{w}}_k|\boldsymbol{\theta}_k) p(\boldsymbol{\theta}_k|\bar{\boldsymbol{w}}_{0:k-1}). \quad (15)$$

One assumption is that the process noise is Gaussian given the noise parameters, hence the likelihood $p(\bar{\boldsymbol{w}}_k|\boldsymbol{\theta}_k)$ in (15) is Gaussian. Therefore, we can utilize the concept of conjugate priors. If a prior distribution belongs to the same family as the posterior distribution, the prior is conjugate to the likelihood. For Normal data $\bar{\boldsymbol{w}} \in \mathbb{R}^d$ with unknown mean $\boldsymbol{\mu}$ and covariance $\boldsymbol{\Sigma}$, a Normal-inverse-Wishart distribution defines the conjugate prior [20], $p(\boldsymbol{\mu}_k, \boldsymbol{\Sigma}_k) := \mathrm{NiW}(\gamma_{k|k}, \hat{\boldsymbol{\mu}}_{k|k}, \boldsymbol{\Lambda}_{k|k}, \nu_{k|k})$. The computation of the statistics $S_{k|k} := (\gamma_{k|k}, \hat{\boldsymbol{\mu}}_{k|k}, \boldsymbol{\Lambda}_{k|k}, \nu_{k|k})$ is done as [15]

$$\gamma_{k|k} = \frac{\gamma_{k|k-1}}{1 + \gamma_{k|k-1}}, \quad (16a)$$
$$\hat{\boldsymbol{\mu}}_{k|k} = \hat{\boldsymbol{\mu}}_{k|k-1} + \gamma_{k|k} \boldsymbol{z}_k, \quad (16b)$$
$$\nu_{k|k} = \nu_{k|k-1} + 1, \quad (16c)$$
$$\boldsymbol{\Lambda}_{k|k} = \boldsymbol{\Lambda}_{k|k-1} + \frac{1}{1 + \gamma_{t|t-1}} \boldsymbol{z}_k \boldsymbol{z}_k^{\mathrm{T}}, \quad (16d)$$
$$\boldsymbol{z}_k = \bar{\boldsymbol{w}}_k - \hat{\boldsymbol{\mu}}_{k|k-1}. \quad (16e)$$

For time-varying parameters, the prediction step consists of

$$\begin{aligned} \gamma_{k|k-1} &= \frac{1}{\lambda} \gamma_{k-1|k-1}, \\ \hat{\boldsymbol{\mu}}_{k|k-1} &= \hat{\boldsymbol{\mu}}_{k-1|k-1}, \\ \nu_{k|k-1} &= \lambda \nu_{k-1|k-1}, \\ \boldsymbol{\Lambda}_{k|k-1} &= \lambda \boldsymbol{\Lambda}_{k-1|k-1}, \end{aligned} \quad (17)$$

where $\lambda \in [0, 1]$ produces exponential forgetting. Further, for a Normal-inverse-Wishart prior, the predictive distribution of the data $\bar{\boldsymbol{w}}$ is a Student-t,

$$\mathrm{St}\left(\hat{\boldsymbol{\mu}}_{k|k-1}, \frac{1 + \gamma_{k|k-1}}{\nu_{k|k-1} - d + 1} \boldsymbol{\Lambda}_{k|k-1}, \nu_{k|k-1} - d + 1\right).$$

Assume that the predictive distribution in (15) is Normal-inverse-Wishart. From (15), also the posterior is Normal-inverse Wishart, $p(\boldsymbol{\theta}_k|\boldsymbol{x}_{0:k}, \boldsymbol{y}_{0:k}) = \mathrm{NiW}(\hat{\boldsymbol{\mu}}_{k|k}, \boldsymbol{\Lambda}_{k|k}, \nu_{k|k})$. In a practical implementation, (16) and (17) are only applied to the process noise, thus decreasing the estimation problem from $d = 6$ do $d_w = 3$. However, to include information from the likelihood into the update of the parameters, $\bar{\boldsymbol{w}}_k$ in (16e) must be generated through the measurement model. We will describe this in more detail in Sec. III-D.

C. Bias Estimation

The bias updates rely on having computed both the posterior for the state trajectory and the noise parameters. Thus, the bias estimation is concerned with computing the posterior $p(\boldsymbol{b}_k|\boldsymbol{\theta}_k, \boldsymbol{x}_{0:k}, \boldsymbol{y}_{0:k})$. First, the prediction model of the bias states is a random walk, see (8), which is linear. Second, the dynamics of the bias states are independent on both the unknown process noise and the vehicle states. Hence, the

Kalman predictor is the optimal predictor, and the prediction step consists of predicting the mean and covariance of the bias state, once per particle. Hence,

$$\hat{\boldsymbol{b}}_{k+1|k} = \hat{\boldsymbol{b}}_{k|k}, \quad \boldsymbol{P}_{k+1} = \boldsymbol{P}_k + \boldsymbol{Q}. \tag{18}$$

For the measurement update, (9) conditioned on the state trajectory and the noise parameters is affine in $\boldsymbol{b}_k$ with known, Gaussian measurement noise $\bar{\boldsymbol{e}}_k$. Hence, the measurement update consists of a Kalman update, again once per particle,

$$\begin{aligned}
\hat{\boldsymbol{b}}_{k|k} &= \hat{\boldsymbol{b}}_{k|k-1} + \boldsymbol{K}_k(\boldsymbol{y}_k - \boldsymbol{h}_k - \boldsymbol{d}_k\hat{\boldsymbol{\mu}}_{k|k} - \hat{\boldsymbol{b}}_{k|k-1}),\\
\boldsymbol{P}_{k|k} &= \boldsymbol{P}_{k|k-1} - \boldsymbol{K}_k\boldsymbol{S}_k^{-1}\boldsymbol{K}_k^{\mathrm{T}},\\
\boldsymbol{K}_k &= \boldsymbol{P}_{k|k-1}\boldsymbol{S}_k^{-1},\\
\boldsymbol{S}_k &= (\boldsymbol{P}_{k|k-1} + \boldsymbol{R} + \hat{\boldsymbol{\Sigma}}_{k|k}).
\end{aligned} \tag{19}$$

D. Algorithm Implementation

In this section, we make connections between the densities in (10) to formulate our joint state and parameter estimation method. Consider first the weight update and measurement likelihood in (13). To compute (14a), from (7) and (9) it is clear that the knowledge of $\boldsymbol{x}_k$ and $\boldsymbol{y}_k$ characterizes $\bar{\boldsymbol{e}}_k$. Combining this with the lemma on transformations of variables in densities [21] gives that

$$p(\boldsymbol{y}_k|\boldsymbol{x}_{0:k}, \boldsymbol{y}_{0:k-1}) \propto p(\bar{\boldsymbol{e}}_k(\boldsymbol{y}_k, \boldsymbol{x}_k)|\bar{\boldsymbol{e}}_{0:k-1}). \tag{20}$$

We marginalize out the noise parameters using the law of total probability as

$$\begin{aligned}
p(\boldsymbol{y}_k|\boldsymbol{x}_{0:k}, \boldsymbol{y}_{0:k-1}) = \int & p(\boldsymbol{y}_k|\boldsymbol{\theta}_k, \boldsymbol{x}_k)\\
&\cdot p(\boldsymbol{\theta}_k|\boldsymbol{x}_{0:k-1}, \boldsymbol{y}_{0:k-1})\,\mathrm{d}\boldsymbol{\theta}_k.
\end{aligned} \tag{21}$$

For $\bar{\boldsymbol{e}}_k = \boldsymbol{d}_k\boldsymbol{w}_k$, (21) is the integral of the product of a Gaussian distribution and a Normal-inverse-Wishart distribution. Hence, (21) is a Student-t distribution [20], implying that

$$p(\bar{\boldsymbol{e}}_k(\boldsymbol{y}_k, \boldsymbol{x}_k)|\bar{\boldsymbol{e}}_{0:k-1}) = \mathrm{St}(\hat{\boldsymbol{\mu}}_{k|k-1}, \tilde{\boldsymbol{\Lambda}}_{k|k-1}, \tilde{\nu}_{k|k-1}),$$

with $\tilde{\nu}_{k|k-1} = \nu_{k|k-1} - 2$, and mean and scaling

$$\begin{aligned}
\hat{\boldsymbol{\mu}}_{\bar{e},k|k-1} &= \boldsymbol{d}_k\hat{\boldsymbol{\mu}}_{k|k-1},\\
\tilde{\boldsymbol{\Lambda}}_{k|k-1} &= \frac{1+\gamma_{k|k-1}}{\tilde{\nu}_{k|k-1}}\boldsymbol{d}_k\boldsymbol{\Lambda}_{k|k-1}\boldsymbol{d}_k^{\mathrm{T}}.
\end{aligned}$$

However, in our case, $\bar{\boldsymbol{e}}_k$ is partially known through the Gaussian distributions $\boldsymbol{e}_k$ and $\boldsymbol{b}_k$, which complicates matters as we have a mixture of Gaussian and Student-t distributions, whose density has no closed form. To obtain an algorithm suitable for online implementation, we relax the Gaussian distribution for the inertial measurements and approximate it as a Student-t through moment matching. This leads to a modified scale parameter in the Student-t as

$$\tilde{\boldsymbol{\Lambda}}_{\bar{e},k|k-1} = \frac{1+\gamma_{k|k-1}}{\tilde{\nu}_{k|k-1}}\boldsymbol{d}_k\boldsymbol{\Lambda}_{k|k-1}\boldsymbol{d}_k^{\mathrm{T}} + \frac{\tilde{\nu}_{k|k-1}-2}{\tilde{\nu}_{k|k-1}}\bar{\boldsymbol{R}}, \tag{22}$$

where $\bar{\boldsymbol{R}} = \boldsymbol{R} + \boldsymbol{P}_{k|k-1}$. The approximation (22) can be interpreted as a robustification of the measurement noise by choosing the smallest common degree of freedom. Furthermore, in stationarity, from $\lim_{\nu\to\infty}\mathrm{St}(\boldsymbol{\mu}, \boldsymbol{\Lambda}, \nu) = \mathcal{N}(\boldsymbol{\mu}, \boldsymbol{\Lambda})$, it follows that we recover the Gaussian measurement noise with precision determined by the forgetting factor. Hence, the measurement update (13) is done by

$$\begin{aligned}
q_k^i &\propto q_{k-1}^i\mathrm{St}(\boldsymbol{\mu}^*, \tilde{\boldsymbol{\Lambda}}^*, \tilde{\nu}),\\
\boldsymbol{\mu}^* &= \boldsymbol{h}_k + \boldsymbol{d}_k\hat{\boldsymbol{\mu}}_{k|k-1} + \boldsymbol{b}_k,\\
\tilde{\boldsymbol{\Lambda}}^* &= \frac{1+\gamma_{k|k-1}}{\tilde{\nu}_{k|k-1}}\boldsymbol{d}_k\boldsymbol{\Lambda}_{k|k-1}\boldsymbol{d}_k^{\mathrm{T}} + \frac{\tilde{\nu}_{k|k-1}-2}{\tilde{\nu}_{k|k-1}}\bar{\boldsymbol{R}}.
\end{aligned} \tag{23}$$

For the prediction step (14b),

$$p(\boldsymbol{x}_{k+1}|\boldsymbol{x}_{0:k}, \boldsymbol{y}_{0:k}) \propto p(\boldsymbol{w}_k(\boldsymbol{x}_{k+1})|\bar{\boldsymbol{e}}_{0:k}). \tag{24}$$

Now, by marginalizing out the noise parameters in (14b), utilizing (22) and combining with (24), we obtain

$$p(\boldsymbol{w}_k(\boldsymbol{x}_{k+1})|\bar{\boldsymbol{e}}_{0:k}) = \mathrm{St}(\hat{\boldsymbol{\mu}}_k^*, \tilde{\boldsymbol{\Lambda}}_k^*, \nu_k^*), \tag{25}$$

where

$$\begin{aligned}
\boldsymbol{\mu}_k^* &= \hat{\boldsymbol{\mu}}_{k|k-1} + \boldsymbol{d}_k\boldsymbol{\Lambda}_{k|k-1}\tilde{\boldsymbol{\Lambda}}_{\bar{e},k|k-1}^{-1}\boldsymbol{z}_k,\\
\tilde{\boldsymbol{\Lambda}}_k^* &= \frac{\nu_{k|k-1} - d + 1 + \boldsymbol{z}_k\tilde{\boldsymbol{\Lambda}}_{\bar{e},k|k-1}^{-1}\boldsymbol{z}_k^{\mathrm{T}}}{\nu_{k|k-1} - d_y + 1}\Big(\boldsymbol{\Lambda}_{k|k-1}\\
&\qquad - \boldsymbol{d}_k\boldsymbol{\Lambda}_{k|k-1}\tilde{\boldsymbol{\Lambda}}_{\bar{e},k|k-1}^{-1}\boldsymbol{\Lambda}_{k|k-1}^{\mathrm{T}}\boldsymbol{d}_k^{\mathrm{T}}\Big),\\
\nu_k^* &= \nu_{k|k-1} - d_w + 1, \quad \boldsymbol{z}_k = \bar{\boldsymbol{e}}_k - \hat{\boldsymbol{\mu}}_{\bar{e},k|k-1}.
\end{aligned}$$

Using the prediction model as proposal density in the particle filter simplifies the algorithm greatly, since we can draw samples from (25), and use these samples both to predict the particles according to (7) and to update the sufficient statistics in (16). Note also that the correlation between process and measurement noise is accounted for by (25). Particle filters can often benefit greatly from an improved proposal distribution $\pi(\cdot)$, but the simplification by using the sampled noise values in both the measurement update of the sufficient statistics and the weight update, is tempting.

Finally, to obtain estimates of the mean and covariance of the process noise, we approximate the marginal as

$$\begin{aligned}
p(\boldsymbol{\theta}_k|\boldsymbol{y}_{0:k}) &= \int p(\boldsymbol{\theta}_k|\boldsymbol{x}_{0:k}, \boldsymbol{y}_{0:k})p(\boldsymbol{x}_{0:k}|\boldsymbol{y}_{0:k})\mathrm{d}\boldsymbol{x}_{0:k}\\
&\approx \sum_{i=1}^N q_k^i p(\boldsymbol{\theta}_k|\boldsymbol{x}_{0:k}^i, \boldsymbol{y}_{0:k}),
\end{aligned} \tag{26}$$

which has complexity $\mathcal{O}(N)$. Based on (26), the unknown parameters can be extracted [12], [14]. To obtain the marginal posterior of the states, we extract the last state from (11),

$$p(\boldsymbol{x}_k|\boldsymbol{y}_{0:k}) \approx \sum_{i=1}^N q_k^i\delta(\boldsymbol{x}_k - \boldsymbol{x}_k^i). \tag{27}$$

Both (26) and (27) overlook a potential path-degeneracy problem, but taking into account different paths often leads to an algorithm that is intractable for online implementation, which is the focus here. Furthermore, for sufficient mixing in the dynamic model (7), errors in the state are forgotten exponentially in time, which ensures convergence of (27) as $N \to \infty$ [11]. For (26), exponential forgetting suppresses the path-degeneracy problem, which causes issues for estimation

of static parameters. The use of exponential forgetting acts as a way to include mixing in the parameter estimation. Algorithm 1 summarizes the method.

Algorithm 1 Bayesian Road-Friction Estimator

Initialize: Set $\{\boldsymbol{x}_0^i\}_{i=1}^N \sim p_0(\boldsymbol{x}_0)$, $\{q_0^i\}_{i=1}^N = 1/N$, $\{S_0^i\}_{i=1}^N = \{\gamma_0^i, \boldsymbol{\mu}_{w,0}^i, \boldsymbol{\Lambda}_{w,0}^i, \nu_0^i\}$, $\{\boldsymbol{b}_0^i\}_{i=1}^N \sim p_0(\boldsymbol{b}_0)$

for $k \leftarrow 0$ to T **do**
  for $i \in \{1, \ldots, N\}$ **do**
    Update weight $\bar{q}_k^i$ using (23).
    Update noise statistics $S_{k|k}^i$ using (16).
  end for
  Normalize weights as $q_k^i = \bar{q}_k^i / (\sum_{i=1}^N \bar{q}_k^i)$.
  Compute $N_{\text{eff}} = 1/(\sum_{i=1}^N (q_k^i)^2)$
  if $N_{\text{eff}} \leq N_{\text{thr}}$ **then**
    Resample particles and copy the corresponding statistics. Set $\{q_k^i\}_{i=1}^N = 1/N$.
  end if
  Approximate state posterior with (27).
  Approximate parameter posterior with (26).
  for $i \in \{1, \ldots, N\}$ **do**
    Measurement update of bias using (19).
    Predict noise statistics $S_{k+1|k}^i$ using (17).
    Sample $\boldsymbol{w}_k^i$ from (25).
    Predict state $\boldsymbol{x}_{k+1}^i$ using (7).
    Predict bias using (18).
  end for
end for

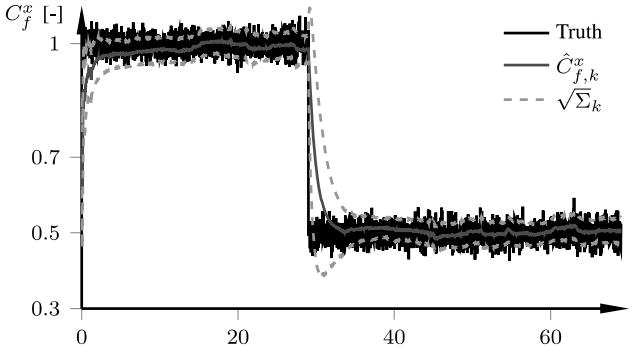

Fig. 1. Estimated normalized longitudinal tire stiffness (red) and associated standard deviation (green) for 500 particles with a forgetting factor of $\lambda = 0.99$, for one realization. Normalized due to confidentiality.

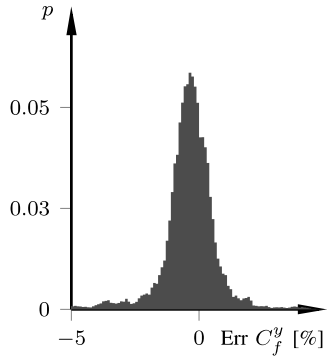

Fig. 2. Histogram of the mean error for the front lateral stiffness, using 500 particles over 100 Monte-Carlo executions. Results are similar for the other stiffness quantities.

IV. Results

A. Simulation Results

To generate synthetic data, we use a single-track model with steering angle and wheel torques as inputs. The inputs are square waves with period time 4 and 5 seconds, respectively, and they are chosen such that the longitudinal wheel slip is below 5% and the small-slip approximations (4) for the wheel-slip angles hold. The tire-stiffness parameters are individually independent and Gaussian distributed with standard deviation approximately 5% of the true values. At 30 seconds, there is a change of road surface. The mean of the initial vehicle state and the initial covariance are $x_0 = [22\ 0\ 0]^{\mathrm{T}}, P_0 = \mathrm{diag}([1\ 1\ \pi/180]^2)$, which are also used to generate the ground truth. The initial standard deviation of the stiffness estimates is 30 % of the true values and the stiffness values are 70% of the true values. The noise values of the measurements are typical for low-cost inertial sensors. The bias is set to zero for simplicity.

Fig. 1 shows stiffness values for one Monte-Carlo trial. The results are similar for the other stiffness quantities. The accuracy of the estimated standard deviation in stationarity in this realization is within 5%.

Fig. 2 display a histogram over the estimated mean of the front lateral stiffness. The plot shows the probability on the y-axis and the error in percentage on the x-axis. The error of the mean value should ideally be Gaussian distributed, since all available information is utilized if the error is Gaussian. Clearly, the error is centered close to zero with the error distribution resembling a Gaussian.

B. Experimental Evaluation

We have used a mid-size SUV, equipped with state-of-the-art validation equipment, to gather data. The parameters of the vehicle model and the tire-stiffness parameters are extracted from data sheets and extensive experimental validation. The dataset consists of an initial accelerating phase followed by a double lane-change maneuver on dry, even asphalt. The vehicle model assumes knowledge of the front-wheel steering angle, which is not measured. However, the angle of the steering wheel, available from the CAN bus, is converted to a steering angle of the front wheel assuming a constant gear ratio. The Normal-inverse-Wishart prior is initialized to have an error in the mean value of 20%, with an initial standard deviation of 30% of the mean value.

Fig. 3 shows normalized mean and standard deviations for the stiffness. In the initial straight-line driving phase (roughly first 10 seconds), the lateral estimates, especially the rear stiffness C_r^y, get insufficient excitation. However, the benefits of including longitudinal dynamics can be seen in the plot for C_f^y, which gets excitation through the longitudinal inputs in the beginning of the data set. The excitation level is small throughout (see Fig. 4), but as soon as the double lane-change

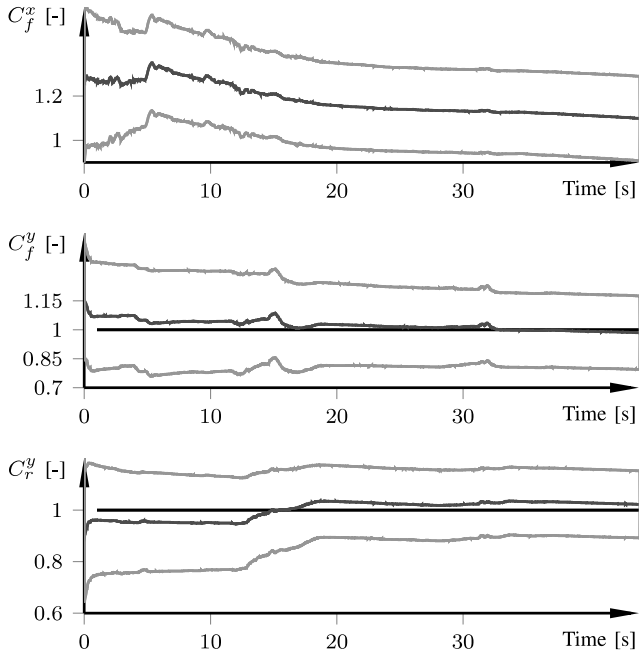

Fig. 3. Estimated normalized tire stiffness (red) and associated standard deviation (green) for 500 particles with $\lambda = 0.995$. Ground truth in black. The coupling effects are clearly seen for C_f^y, which starts to converge despite virtually no steering in the beginning.

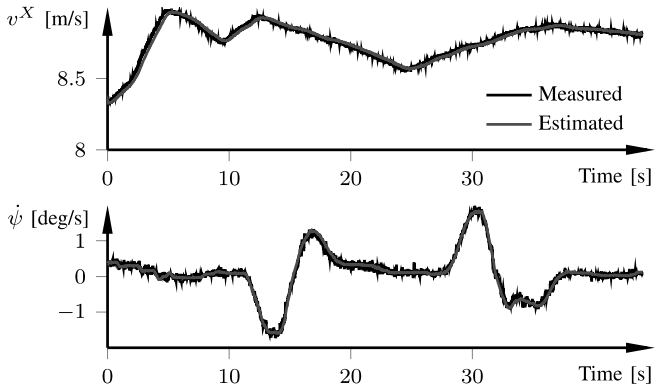

Fig. 4. Estimated longitudinal velocity and yaw rate. Ground truth for the lateral velocity was not available for this experiment.

maneuver is initiated, around 13 seconds, the lateral stiffness estimates start to find the correct values. There is no ground truth available for the longitudinal stiffness, but the estimated values are reasonable throughout the experiments.

Fig. 4 displays the estimated and measured longitudinal velocity and yaw rate, for which we have ground truth. Both the longitudinal velocity and yaw rate are closely tracked throughout. Note the small acceleration and yaw-rate values, indicating that there is only a small level of excitation in the system. Despite this, the parameters can be estimated with high precision. For example, the average error of the front lateral stiffness throughout the experiment is 2.2%, and the same number for the rear lateral stiffness is 0.2% (Fig. 3).

V. Conclusion

We presented a novel approach to joint state and tire-stiffness estimation using inertial and wheel-speed sensors. The resulting vehicle model leads to dependence between the unknown process noise and the measurement noise. We proposed a computationally efficient method to handle the dependence. The method relies on conjugate priors and moment matching to obtain a computationally efficient marginalized particle filter, and by using exponential forgetting in the parameter prediction, we can handle time-varying road conditions. Preliminary experimental results are highly promising. It is future work to fully evaluate the algorithm on longer data sets, under varying road conditions.

References

[1] K. Berntorp, B. Olofsson, K. Lundahl, and L. Nielsen, "Models and methodology for optimal trajectory generation in safety-critical road–vehicle manoeuvres," *Vehicle System Dynamics*, vol. 52, no. 10, pp. 1304–1332, 2014.

[2] F. Gustafsson, "Slip-based tire-road friction estimation," *Automatica*, vol. 33, pp. 1087–1099, 1997.

[3] C. R. Carlson and J. C. Gerdes, "Consistent nonlinear estimation of longitudinal tire stiffness and effective radius," *IEEE Trans. Contr. Syst. Technol.*, vol. 13, no. 6, pp. 1010–1020, 2005.

[4] S. Di Cairano, H. Tseng, D. Bernardini, and A. Bemporad, "Vehicle yaw stability control by coordinated active front steering and differential braking in the tire sideslip angles domain," *IEEE Trans. Contr. Syst. Technol.*, vol. 21, no. 4, pp. 1236–1248, 2013.

[5] C. Lundquist and T. B. Schön, "Joint ego-motion and road geometry estimation," *Information Fusion*, vol. 12, no. 4, pp. 253–263, 2011.

[6] C. Lundquist and T. B. Schön, "Recursive identification of cornering stiffness parameters for an enhanced single track model," in *15th IFAC Symp. System Identification*, Saint-Malo, France, July 2009.

[7] C. Canudas-de Wit and R. Horowitz, "Observers for tire/road contact friction using only wheel angular velocity information," in *38th IEEE Conf. Decision and Control*, Phoenix, AZ, Dec. 1999.

[8] G. Baffet, A. Charara, and D. Lechner, "Estimation of vehicle sideslip, tire force and wheel cornering stiffness," *Control Eng. Pract.*, vol. 17, no. 11, pp. 1255–1264, 2009.

[9] R. Wang and J. Wang, "Tire-road friction coefficient and tire cornering stiffness estimation based on longitudinal tire force difference generation," *Control Eng. Pract.*, vol. 21, no. 1, pp. 65–75, 2013.

[10] C. Sierra, E. Tseng, A. Jain, and H. Peng, "Cornering stiffness estimation based on vehicle lateral dynamics," *Vehicle System Dynamics*, vol. 44, no. 1, pp. 24–38, 2006.

[11] A. Doucet and A. M. Johansen, "A tutorial on particle filtering and smoothing: Fifteen years later," in *Handbook of Nonlinear Filtering*, D. Crisan and B. Rozovsky, Eds. Oxford University Press, 2009.

[12] T. B. Schön, F. Gustafsson, and P.-J. Nordlund, "Marginalized particle filters for mixed linear nonlinear state-space models," *IEEE Trans. Signal Processing*, vol. 53, pp. 2279–2289, 2005.

[13] C. M. Bishop, *Pattern Recognition and Machine Learning*. NJ, USA: Springer-Verlag New York, 2006.

[14] K. Berntorp and S. Di Cairano, "Process-noise adaptive particle filtering with dependent process and measurement noise," in *55th IEEE Int. Conf. Decision and Control*, Las Vegas, NV, Dec. 2016.

[15] E. Özkan, V. Šmídl, S. Saha, C. Lundquist, and F. Gustafsson, "Marginalized adaptive particle filtering for nonlinear models with unknown time-varying noise parameters," *Automatica*, vol. 49, no. 6, pp. 1566–1575, 2013.

[16] K. Berntorp, "Joint wheel-slip and vehicle-motion estimation based on inertial, GPS, and wheel-speed sensors," *IEEE Trans. Contr. Syst. Technol.*, vol. 24, no. 3, pp. 1020–1027, 2016.

[17] E. Schindler, *Fahrdynamik: Grundlagen Des Lenkverhaltens Und Ihre Anwendung Für Fahrzeugregelsysteme*. Renningen, Germany: Expert-Verlag, 2007.

[18] F. Gustafsson, *Statistical Sensor Fusion*. Lund, Sweden: Utbildningshuset/Studentlitteratur, 2010.

[19] S. Saha and F. Gustafsson, "Particle filtering with dependent noise processes," *IEEE Trans. Signal Processing*, vol. 60, no. 9, pp. 4497–4508, 2012.

[20] K. P. Murphy, "Conjugate Bayesian analysis of the Gaussian distribution," UBC, Tech. Rep., 2007.

[21] C. R. Rao, *Linear Statistical Inference and its Applications*. Wiley, 2001.